Published in final edited form as:
J Pharm Sci. 2012 July ; 101(7): 2353–2363. doi:10.1002/jps.23127.

MRI Study of Subconjunctival and Intravitreal Injections

S. KEVIN LI[1], **JINSONG HAO**[1], **HONGSHAN LIU**[2], and **JING-HUEI LEE**[3]

[1]Division of Pharmaceutical Sciences, James L. Winkle College of Pharmacy, University of Cincinnati, Cincinnati, Ohio 45267

[2]Department of Ophthalmology, College of Medicine, University of Cincinnati, Cincinnati, Ohio 45267

[3]School of Energy, Environmental, Biological, and Medical Engineering, College of Engineering and Applied Science, University of Cincinnati, Cincinnati, Ohio 45267

Abstract

Previous magnetic resonance imaging (MRI) studies to investigate the routes of penetration and barriers in ocular delivery have provided insights into the mechanisms of transscleral and intraocular drug delivery. The objective of the present study was to investigate ocular penetration and clearance after subconjunctival and intravitreal injections using a contrast agent at concentrations higher than those in the previous studies. This high concentration approach was hypothesized to allow the visualization of the contrast agent in the eye that could not be achieved previously. Subconjunctival and intravitreal injections of contrast agent Magnevist, a model hydrophililc probe, were performed in rabbits, and the distribution and clearance of the probe after the injections were examined by MRI. After subconjunctival injection *in vivo*, significant contrast agent penetration into the anterior chamber was observed but not into the vitreous. A clearance pathway of the hydrophilic probe from the subconjunctival depot to the regions near the periocular fat behind the eye was found. After intravitreal injection *in vivo*, the contrast agent was observed in the anterior chamber, optic nerve, and tissues surrounding the eye during clearance. MRI continues to provide insights into the transport barriers and clearance pathways of hydrophilic molecules in ocular delivery.

Keywords

ophthalmic drug delivery; pharmacokinetics; distribution; clearance; subconjunctival injection; transscleral delivery; intravitreal injection; imaging methods; MRI; transport

INTRODUCTION

Patients suffering from posterior eye diseases are in need of therapies with effective methods to deliver drugs to the back of the eye. The common methods of topical administration of eye drops cannot effectively deliver drugs to the posterior segment of the eye. Systemic drug delivery to achieve therapeutic levels of drugs in the eye usually leads to unwanted systemic side effects. Intravitreal injection is effective and widely used in posterior eye disease treatment, but repeated administration is often required that leads to complications such as vitreous hemorrhage, retinal detachment, and endophthalmitis. A robust and convenient drug delivery platform for posterior eye diseases is currently not available. This is partly due to

Correspondence to: S. Kevin Li (Telephone: +513-558-0977; Fax: + 513-558-4372; kevin.li@uc.edu).

the lack of understanding of the ocular drug delivery barriers, distribution, and clearance in the eye.

The mechanisms of ocular drug delivery and clearance are complicated. Traditional pharmacokinetic studies of eye dissection have yielded important information of these mechanisms, but the traditional pharmacokinetic approaches have limitations.[1] Magnetic resonance imaging (MRI) is a noninvasive method and can be used to study the mechanisms of ocular drug delivery. Previous studies have demonstrated the utility of MRI to characterize the routes of penetration and ocular barriers such as the dynamic barriers, least resistive route of transscleral penetration, drug delivery flux-enhancing mechanisms, locations of periocular and intraocular depots, and release kinetics from these depots (or ocular implants) in periocular, intrascleral, suprachoroidal, and intravitreal delivery.[2-10] Such information would be difficult to obtain in traditional pharmacokinetic studies involving the dissection of the eye in ocular delivery research.

Previous MRI studies of ocular delivery used contrast agents such as gadopentetate dimeglumine [gadolinium (Gd)–diethylene triamine pentaacetic acid (DTPA); Magnevist], manganese ion (Mn^{2+}), Mn–ethylenediaminetetraacetate (Mn–EDTA), and Gd–albumin (Galbumin) as hydrophilic probes typically at concentrations near the peaks of the MR signal versus concentration curves or at concentrations up to around 0.1 M. In MRI studies of transscleral delivery, subconjunctival administration[3,5] and episcleral implant[2] *in vivo* were not able to deliver significant amounts of contrast agents into the anterior chamber, and no contrast agent penetration into the vitreous was observed. Although the inability to detect contrast agent in the eye in these MRI studies suggests low efficiency of intraocular delivery through the subconjunctival route, these results could also be related to the sensitivity of the MRI techniques as a result of the contrast agent concentrations used in these ocular delivery studies and the concentration resulted from the slow release rate of the contrast agent in the ocular implant study. In addition, MRI was not able to visualize the clearance pathways from the subconjunctival space, except an increase in the contrast signal at the buccal lymph node, possibly due to the contrast agent concentration in and the dimensions of the blood and lymph vessels.[2] In MRI studies of intravitreal injection[4,8,9] and intraocular implant,[2,11] contrast agents were not detected at the level that can be quantified in the anterior chamber with the MRI techniques. There was also no identifiable elimination pathway from the vitreous after intravitreal administration, probably due to the limitations of the MRI studies as described above. Methods to improve the detection of contrast agent in ocular MRI studies include increasing the contrast agent concentration and following signal intensity changes with correlation image maps.[12] These methods have not been employed in the visualization of ocular delivery and clearance in ocular pharmacokinetic studies using MRI.

The objective of the present study was to investigate the distribution of hydrophilic ionic compounds after subconjunctival and intravitreal injections. MRI experiments were performed at Gd–DTPA concentration from 0.005 to 0.5 M to study the transport barriers and clearance pathways related to these two methods of ocular drug delivery. Particularly, the following questions raised in previous MRI studies were to be addressed. What contrast agent concentration is required in subconjunctival injection to provide significant intraocular penetration into the anterior chamber to be studied using MRI? Can high contrast agent concentration in subconjunctival injection provide detectable transscleral delivery of the agent into the vitreous? What are the clearance pathways of the hydrophilic probe from the subconjunctival depot? In intravitreal injection, what is the distribution of the contrast agent in the vitreous and anterior chamber, for example, the concentration of the hydrophilic probe in the anterior chamber relative to that in the vitreous as a result of vitreal clearance via the anterior chamber? What are the clearance paths for the hydrophilic probe in the vitreous

after intravitreal injection? Understanding the transport barriers and clearance pathways in ocular delivery would be helpful in designing an effective ocular drug delivery system.

EXPERIMENTAL

Materials

Contrast agent Magnevist from Bayer HealthCare Pharmaceuticals Inc. (Wayne, New Jersey) was used as a model hydrophilic compound in the present study. Sodium chloride (NaCl) was purchased from Arcos Organics (Geel, Belgium) and used to prepare 0.9% NaCl solution (saline) using distilled deionized water. Various concentrations of Gd–DTPA solutions were prepared by the dilution of Magnevist with saline. The pH of Gd–DTPA solutions was checked and found to be between pH 6 and 7.

MRI Calibration

Experiments were conducted to study the relationship between MR signal and Gd–DTPA concentration ranging from 0.01 mM to 0.5 M in saline. MRI experiments were performed in a clinical 3-T MRI system (GE Signa Excite, Milwaukee, Wisconsin). The solutions were prepared in 3 mL vials and imaged with T_1 weighted spin–echo pulse sequences: repetition time (TR) of 800 ms, echo time (TE) of 13 ms, and fat suppression. Prescanning was performed at the beginning of each experiment. Coronal MR images were obtained and analyzed with ImageJ (NIH, Bethesda, Maryland) and/or Photoshop (Adobe Systems, San Jose, California). An MR signal intensity enhancement versus Gd–DTPA concentration plot was constructed and used as the calibration curve in the quantitation of the contrast agent in the aqueous humor.

The signal in spin–echo imaging can be described by:

$$S_1 = S_0 \left[1 - \exp\left(-\frac{TR}{T_1}\right)\right]\left[\exp\left(-\frac{TE}{T_2}\right)\right] \quad (1)$$

where S_I is the signal intensity, S_0 is the intrinsic fully recovered signal intensity, T_1 is the spin–lattice relaxation time constant, and T_2 is the spin–spin relaxation time constant. T_1 and T_2 are related to the concentration of the contrast agent:

$$\frac{1}{T_1} = r_1 C + b_1 \quad (2)$$

$$\frac{1}{T_2} = r_2 C + b_2 \quad (3)$$

where C is the concentration of the contrast agent, r_1 and r_2 are the relaxivities of the contrast agent that measure the extent of the contrast agent affecting the T_1 and T_2 relaxation rates of ^1H_2O, and b_1 and b_2 are the intrinsic $1/T_1$ and $1/T_2$ values without the contrast agent, respectively. In the present study, r_1 and r_2 were determined by curve fitting of the MR signal data using Scientist software (MicroMath, Utah) and Eqs. 1-3.

Because of the high contrast agent concentration used in the experiments, the effects of magnetic susceptibility artifact were investigated using 3 mL vials of 0.05–0.5 M contrast agent solutions submerged in saline inside 20 mL vials (see diagram in *Results* section).

Subconjunctival and Intravitreal Injection MRI Studies *In Vivo*

New Zealand white rabbits of 2–4 kg were purchased from Myrtle Rabbitry (Thompsons Station, Tennessee) and Harlan Laboratories (Indianapolis, Indiana) and were used in the experiments under the approval of the Institutional Animal Care and Use Committee at the University of Cincinnati (Cincinnati, Ohio). All experiments were conducted in adherence to the Association for Research in Vision and Ophthalmology Statement for the Use of Animals in Ophthalmic and Vision Research. The rabbits were anesthetized with intramuscular injection of ketamine and xylazine (25–50 mg/kg and 5–10 mg/kg, respectively) or inhalation of isoflurane (1%–5%) depending on the duration of the experiments. Under anesthesia, subconjunctival and intravitreal injections of 0.1 mL Gd–DTPA solutions were performed with 0.5 inch 30-gauge needles at the superior bulbar conjunctiva and the pars plana approximately 3 mm from the corneal limbus, respectively. The concentrations of Gd–DTPA in the solutions were from 0.005 to 0.5 M.

Magnetic resonance imaging experiments were conducted in the clinical 3-T MRI system with a human wrist coil (transmit/receive volume coil). The animals were anesthetized or reanesthetized before each scan. T_1 weighted spin–echo imaging was performed similar to that described in the *MRI Calibration* section and with imaging field of view of 90 mm, 80% phase encoding, 256 readout matrix, 6 signal averages to increase signal-to-noise ratio, and fat suppression unless otherwise stated. The slice thickness was 1.0 mm with no spacing, resulting in spatial resolution of $0.35 \times 0.35 \times 1.0\ mm^3$. Each scan provided at least 20 transaxial image slices to cover the whole eye. Imaging time for a single scan was approximately 16 min.

In the analyses of the MR images, the concentration of the contrast agent in the region of interest (ROI) such as in the aqueous humor was determined by the average MR signals in the ROI and the signal versus concentration calibration curve in *MRI Calibration* section. Here, the exchange of tissue ^1H_2O molecules among compartments was assumed to have little impact on relaxation time constants and relaxivities that were determined in the measurements with the vials.

Subconjunctival Injection MRI Studies Postmortem

The postmortem studies were to assess the ocular delivery barriers without clearance (e.g., vasculature and lymphatic clearance) and to serve as a control in the ocular clearance pathway investigation. The procedure of the postmortem studies was the same as that described for the *in vivo* studies except that the animals were sacrificed with intravenous injection of pentobarbital (100–200 mg/kg; Euthosol, Virbac Corp., Fort Worth, Texas) immediately before the experiments.

RESULTS

MRI Calibration

Gd–DTPA is an ion complex of paramagnetic ion Gd^{3+} and chelate DTPA with a binding constant of approximately 10^{18} /M at pH 7.4 (Bayer Healthcare Pharmaceuticals Inc.). The ion complex has molecular weight of 546 g/mol and net negative charges of $z = -2$. Figure 1 presents the relationship between MR signal ratios of Gd–DTPA solutions to saline and Gd–DTPA concentrations in saline, and the best-fit line for the data using Eqs. 1-3. The best-fitting parameters of Gd–DTPA relaxivities (r_1 and r_2) calculated from the data in the figure were 3 and 5 /mM/s, respectively. These values are within the relaxivity ranges at 37°C reported in the literature.[13-15] From the figure, it was estimated that the detection limit of the contrast agent in the present MRI study was approximately 0.02 mM and the signal approached a maximum at approximately 2 mM Gd–DTPA.

Figure 2 shows the representative MR images of the vials with high Gd–DTPA concentrations enclosed in the larger saline vials to study the effects of magnetic susceptibility artifact. The high Gd–DTPA concentrations create an artifact (i.e., a dark ring) around the inner vials (e.g., 0.05 M) in the MR images. As Gd–DTPA concentration increases, the effects amplify, creating some spatial distortion in addition to signal dropout. Therefore, the concentration of Gd–DTPA used in the present subconjunctival and intravitreal injections would initially produce low MR signals (dark region) in the images at the injection sites in the subconjunctival and intravitreal injection studies.

Subconjunctival Injection

Figure 3 shows the representative MR image before the administration of the contrast agent (control). The MR image obtained using the MR sequence without fat suppression is also presented for comparison, which provides information on the location of periocular fat. Figure 4 presents the representative MR images of rabbit eyes after subconjunctival injections of Gd–DTPA at concentration of 0.05 and 0.5 M *in vivo*. The MR images in the subconjunctival studies postmortem under similar conditions are shown in Figure 5. The dark subconjunctival depot and the corresponding artifact effect around the depot initially were a result of the high Gd–DTPA concentration in the subconjunctival space. As can be seen in Figure 4, penetration of the hydrophilic probe into the ciliary body and anterior chamber was observed within 20 min after the injection. The enhanced signal at the ciliary body away from the subconjunctival depot (e.g., inferior ciliary body) suggests the involvement of local blood circulation in contrast agent delivery in the anterior segment of the eye. Using the MR signal in the aqueous humor, the average concentration of Gd–DTPA in the anterior chamber was determined to be in the range from approximately 0.05 to 0.15 mM at approximately 40 min after the 0.5 M Gd–DTPA injection. Assuming that the volume of the anterior chamber in rabbits is 0.3 mL, the concentration of Gd–DTPA in the anterior chamber corresponds to an amount equal to approximately 0.06% of the Gd–DTPA in the subconjunctival injection solution used in the study. No significant transscleral penetration of Gd–DTPA from the subconjunctival depot into the vitreous was observed after the injection; the contrast agent concentration in the vitreous was below the detection limit of the MRI technique even at the high concentration dose (0.5 M) of the injection. Diffusion of the hydrophilic probe from the subconjunctival depot to the tissues surrounding the eye and a distinctive clearance pathway in the region near the periocular fat behind the eye were also observed in the images.

In the postmortem subconjunctival injection studies, Gd–DTPA was observed to penetrate the ciliary body and anterior chamber from the subconjunctival depot (Fig. 5), similar to the *in vivo* studies (Fig. 4). At approximately 40 min after the injection of 0.5 M Gd–DTPA, the aqueous humor signal corresponds to average concentration of around 0.3 mM or an amount around 0.2% of the Gd–DTPA used in the injection. However, different from the observation in the *in vivo* studies, there was no initial significant increase in the signal of the inferior ciliary body away from the subconjunctival depot. Also, different from the *in vivo* studies was transscleral penetration of the contrast agent into the vitreous after subconjunctival injection postmortem as indicated by the high concentration contrast agent region (shown as the low signal dark region) in the image expanding in the direction toward the center of the globe, reaching deeper into the vitreous over time after the injection. This spreading of the dark area is consistent with contrast agent diffusion to the tissues surrounding the subconjunctival depot. No distinct clearance pathway from the subconjunctival depot near the periocular fat behind the eye was observed, which is different from the observation *in vivo*. As expected, another major difference between the MR images postmortem and *in vivo* was the rate of decrease of contrast agent concentration in the

subconjunctival depot postmortem and *in vivo*. Contrast agent clearance from the subconjunctival site postmortem was significantly slower than that *in vivo*.

The present MRI data allow the assessment of the effect of ocular clearance upon subconjunctival delivery of hydrophilic molecules *in vivo*. Using the postmortem data and assuming the anterior chamber as a single compartment, the apparent rate of the hydrophilic probe delivered to the anterior chamber from the subconjunctival depot was estimated to be approximately 4×10^{-5} mol/s after the 0.5 M Gd–DTPA injection. For comparison, the apparent rate of subconjunctival delivery of the probe to the anterior chamber *in vivo* was approximately 1×10^{-5} mol/s under the same injection condition. The approximately fourfold difference between the observed rates of subconjunctival delivery postmortem and *in vivo* is likely attributed to ocular clearance.

The apparent permeability coefficient (P) related to the barrier of subconjunctival delivery to the anterior chamber can also be estimated using the postmortem data without clearance:

$$P = \frac{Q}{t} \times \frac{1}{AC_D} \quad (4)$$

where P is the apparent permeability coefficient of the tissue barrier, A is the diffusional surface area, Q is the amount of the contrast agent in the anterior chamber, t is time, and C_D is the concentration of the contrast agent in the subconjunctival depot. Assuming that the effective surface area for transscleral transport was 0.1 cm^2, the apparent permeability coefficient estimated was 7×10^{-7} cm/s, which was smaller than the permeability coefficient values of excised sclera for small hydrophilic permeants determined using diffusion cells in previous *in vitro* studies.[16,17]

Intravitreal Injection

Figure 6 presents the representative MR images in the intravitreal injection studies of Gd–DTPA at concentrations of 0.005, 0.05, and 0.5 M *in vivo*. Significant Gd–DTPA distribution from the vitreous to the anterior chamber was found in less than 4 h after the injection. The lower vitreous MR signals (darker) in the 0.5 M intravitreal injection experiments than those after 0.005 and 0.05 M Gd–DTPA injections were due to the higher contrast agent concentration in the vitreous after the 0.5 M injection (MR signal begins to decrease with increasing concentration > 2 mM). In addition to the anterior chamber, other intraocular tissues such as the ciliary body also show enhanced MR signals, indicating the presence of Gd–DTPA in these tissues or compartments in the eye. However, the lens (inside of the lens) was not significantly affected by the contrast agent even with its close proximity to the vitreous. Gd–DTPA was also observed in the tissues surrounding the eye at 4 and 12 h after intravitreal administration. Particularly, the MR signals in the optic nerve region were enhanced, suggesting the presence of the contrast agent in this region during clearance from the vitreous. The presence of Gd–DTPA in the surrounding tissues outside the eye after intravitreal injection initially can be due to leakage of the contrast agent from the injection site at the sclera. The enhanced signals in the surrounding tissues away from the injection site at later time points (e.g., 12 h after the injection) are possibly a result of contrast agent clearance from the vitreous.

To study the clearance of hydrophilic compounds in the vitreous, the distribution of the contrast agent in the vitreous and anterior chamber after the injection was examined. The average concentrations of Gd–DTPA in the anterior chamber at 4 h after intravitreal injection increased when the contrast agent concentration of the injection increased from 0.005 to 0.5 M. The contrast agent concentrations in the anterior chamber were estimated to be 0.1, 0.4, and 2.5 mM at 4 h after the 0.005, 0.05, and 0.5 M injections, respectively.

These anterior chamber concentrations correspond to approximately 10% of those in the vitreous at the MRI time point.

DISCUSSION

Subconjunctival Delivery and Clearance

Previous investigations of the subconjunctival route using MRI have suggested that this route of administration generally could not deliver significant amounts of contrast agents to the anterior chamber for the quantification of the contrast agent probes using MRI *in vivo*.[2,5] The penetration of contrast agents into the anterior chamber was observed only with enhanced delivery using iontophoresis *in vivo* or only in postmortem studies when the dynamic barrier was not present. In the present study at the contrast agent concentration used, the delivery of a significant amount of the contrast agent to the anterior chamber through subconjunctival injection was observed *in vivo* for the first time. It is believed that the contrast agent was initially delivered to the ciliary body, likely by diffusion, and then into the anterior chamber, possibly via blood circulation around the ciliary body structure. This suggests passive permeation from the subconjunctival space at high enough concentration can provide the thermodynamic driving force that overcomes the ocular barriers for the delivery of polar/ionic compounds into the anterior segment of the eye.

No significant transscleral penetration of the contrast agent into the vitreous was observed even at the high contrast agent concentration used in the present *in vivo* study. This is in contrast to the results in the postmortem study showing penetration of the contrast agent into the vitreous. These results are consistent with the more resistive barrier (e.g., retinal pigment epithelium) for intraocular penetration to the posterior segment of the eye than the anterior of the eye[5] and the strong dynamic barrier associated with lymphatic and/or blood vasculature clearance in transscleral delivery.[18] The lower extent of ocular delivery into the posterior segment than into the anterior of the eye in general is believed to be a result of these two factors. For polar/ionic compounds, subconjunctival injection mainly provides ocular delivery to the ciliary body and anterior chamber.

The significance of the dynamic barrier and lymph clearance in transscleral delivery was recently discussed.[2,18,19] Although the principal elimination pathways after subconjunctival administration of the contrast agent were not specifically identified, the observed accumulation of the contrast agent in the buccal lymph node[2] suggested the involvement of lymphatic clearance as a potential ocular drug delivery barrier. A recent study using fluorescein and dyes in rats indicates that at least around 5% of the fluorescein was cleared through the lymphatic system after subconjunctival administration.[20] In the present study, the distribution of Gd–DTPA, an ionic hydrophilic compound, to the surrounding tissues of the eye near the subconjunctival depot and periocular fat behind the eye after subconjunctival injection shows that a significant portion of the compound administered through the periocular route (particularly subconjunctival injection) was distributed to the surrounding tissues and fat. A clearance pathway near the periocular fat behind the eye was also identified for Gd–DTPA *in vivo* that was not observed in the postmortem studies. The observation of a large amount of the contrast agent delivered to the surrounding tissues outside the globe rather than in the eye after subconjunctival administration is consistent with previous findings. For example, an investigation of peribulbar injection of dexamethasone showed high drug plasma concentration in systemic circulation following the injection, and the plasma level was comparable to a “high” systemic oral dose of dexamethasone.[21] Subconjunctival delivery can lead to relatively high systemic drug concentrations (e.g., Refs. 22-25). It is believed that the drug from the injection site does not unidirectionally diffuse into the globe but to the surrounding tissues and systemic circulation via the capillaries and vasculature surrounding the eye.

Intravitreal Delivery and Clearance

It is a general view that drugs in the vitreous can be eliminated through the retina-choroid layer surrounding the vitreous and/or the aqueous humor out-flow pathways in the anterior of the eye.[26,27] For small lipophilic molecules, the predominant route of clearance is suggested to be through the retina in the posterior segment of the eye. For polar molecules and macromolecules, it has been hypothesized that clearance is predominantly through the anterior clearance route. Previous MRI studies of ocular drug delivery have investigated the clearance of contrast agents from the vitreous[2,8,9,11] but did not find significant amounts of contrast agents (or significant increase in MR signal) in the anterior chamber. In addition, no contrast agent was observed in the tissues surrounding the eye or in the optic nerve.

In the present *in vivo* study, when high concentration of Gd–DTPA was used, the MR images show significant distribution of the contrast agent into the anterior chamber. This suggests clearance through the anterior chamber after intravitreal administration of polar compounds. When lower contrast agent concentration was used such as in 0.005 M intravitreal injection, less Gd–DTPA was detected in the anterior chamber, similar to those observed in previous studies.[4,8,9] The present study provided additional evidence to support the anterior route being a clearance pathway for polar molecules that has not been shown in previous MRI studies. A finding in the present study that had not been observed previously was the presence of the contrast agent in the tissues around the eye after intravitreal injection. This suggests diffusion of the hydrophilic probe from the vitreous to these tissues during clearance. One possible route of clearance can be through the injection site at the sclera. Clearance can also occur by diffusion from the vitreous via the retina, choroid, and sclera to the tissues surrounding the eye. The contrast agent can also travel from the vitreous to the periocular tissues through the anterior chamber and then the trabecular meshwork and scleral venous plexus. Another interesting finding was the presence of the contrast agent in the optic nerve after intravitreal injection. The uptake of small contrast ions to the optic nerve after intravitreal administration was previously reported. For example, Mn^{2+} ion was used to visualize the optic projection from the retina to the cortex[28-30] due to the similar characteristics between calcium ion and Mn^{2+} that they can be taken up by retinal ganglion cells through voltage-gated calcium channels from the vitreous. However, the use of contrast chelates such as Gd–DTPA to enhance optic pathway visualization is not common. The result in the present study suggests that hydrophilic molecules diffuse into optic nerve region after intravitreal injection and a small portion of the molecules can leave through this potential clearance route.

Other Considerations in MRI Pharmacokinetic Study

Although the present high Gd–DTPA concentration experiments have provided additional insights into the mechanisms of the penetration route and clearance of subconjunctival and intravitreal delivery, the limitations in these MRI experiments should be discussed. First, as the molecular size of a molecule directly affects its diffusion, membrane penetration, and hence ocular distribution and clearance of the molecule, the present results might not be representative of drugs of molecular sizes significantly different from Gd–DTPA. In addition to molecular size, the lipophilicity of a molecule can also affect tissue partitioning and penetration of the molecule. There can be significant differences in the distributions and pharmacokinetics of the contrast agent and lipophilic molecules in ocular drug delivery. For example, the contrast probe Gd–DTPA in the present study has molecular size larger than those of Mn^{2+} and Mn–EDTA in previous studies[5-7] but smaller than that of Gd–albumin in other studies.[3,8] Gd–DTPA and similar contrast agents have been used as ionic hydrophilic probes in previous MRI ocular pharmacokinetic studies.[2,3,11,31,32] In these MRI studies and the present study, the results of contrast agents such as Gd–DTPA are only representative to ocular pharmacokinetics of polar molecules of similar molecular sizes.

Second, the concentrations of the contrast agent injected were at a level significantly higher than those of the drugs usually used in eye disease treatments. The extrapolation of the present results of high contrast agent concentration to polar drug molecules at low concentration would only be appropriate when linear pharmacokinetics is assumed, for example, no involvement of saturable kinetics such as active transport across ocular tissues.

Third, although Gd–DTPA was typically administered through injection (or infusion) in MRI procedure at the same concentration as those of the highest concentration used in the present study, the high contrast agent concentration might affect the ocular tissue barriers and hence the distribution of the contrast agent in and around the eye after subconjunctival and intravitreal injections. Because of the high Gd–DTPA concentration, the high osmolality of the injected solution can also result in epithelial cell damages. For example, in a cytotoxicity study using an epithelial cell line, 50% cells were damaged in 24 h incubation with 0.125 M Gd–DTPA or mannitol solution of equivalent osmolality.[33] In another study, the 50% lethal dose of Gd–DTPA was found to be 5.6 mmol/kg in mice.[34] Assuming a volume of distribution of 0.2 L/kg,[35] this suggests that the concentration leading to toxicity can be as low as 0.03 M. For the intravitreal injection in the present study, the average contrast agent concentration in the vitreous was below this limit as a result of its dilution and clearance in the vitreous humor after the injection. For the subconjunctival injection, a separate histology experiment performed in mice using 0.5 M Gd–DTPA and whole-mount fluorescence confocal microscopy showed that there was no observable damage to the cornea 20 min after the injection as compared with untreated cornea as a control (unpublished results). In addition, topical application of 0.5 M Gd–DTPA on the eye also showed no sign of toxicity and damage to the cornea. These results suggest that the concentration used in the present study did not damage epithelial cell layers such as the cornea and lead to enhanced Gd–DTPA penetration into the anterior chamber.

Even though Gd–DTPA did not show any toxicity effects to the epithelial tissue, an increase in tissue permeability due to the high concentration of Gd–DTPA cannot be excluded. Particularly, the excess free DTPA in Magnevist may bind to divalent cations (e.g., Ca^{2+} ions) in tissues and affect their barrier properties. For example, chelating agents such as EDTA can interact with tight junctions of epithelial cells and enhance paracellular transport across epithelium.[36] DTPA may possess similar tissue barrier modifying properties as EDTA.

Another limitation of the present study is the validity of the postmortem results. It is unclear as to how long the eye tissues remain viable after the animals are sacrificed in the postmortem experiments. Possible tissue barrier degradation can compromise the results and the interpretation of the data. For instance, some investigators have proposed that eye tissues such as retinal pigmented epithelium could remain intact several hours postmortem,[2,20] but others have suggested that the blood retina barrier (e.g., endothelial cell tight junctions) could be altered within hours after animal death.[37] Therefore, caution must be exercised in the interpretation of the postmortem results due to potential postmortem tissue changes.

Lastly, temperature can affect the diffusion coefficients of molecules and relaxivities of ^1H_2O MR.[38,39] Diffusion coefficients of ions increase by approximately 30% from 25°C to 37°C in saline and the difference in relaxivities at these temperatures can result in up to 20% change in MR signals at Gd–DTPA concentration in the 0–20 mM range. Thus, the lower body temperature postmortem than *in vivo* can influence the comparison of the *in vivo* and postmortem MRI results, but such effects, for example, on relaxivity, due to the changes in molecular motion from body to room temperature generally are not significant.

CONCLUSION

Previous studies have demonstrated the utility of MRI to investigate the routes of penetration, transport barriers, and clearance pathways of ocular delivery, and the mechanisms of transscleral and intraocular drug delivery systems. The present study investigated the distribution of a contrast agent (as a hydrophilic ionic probe) after subconjunctival and intravitreal injections to study a number of questions raised related to the observations in previous MRI studies. It was believed that using a contrast agent at higher concentration than those in these previous studies could be useful in visualizing the contrast agent in the penetration and clearance pathways to address these questions. The following are the main findings in the present study. Different from the previous MRI studies, significant intraocular penetration into the anterior chamber was observed after subconjunctival injection *in vivo*. This difference is due to the high contrast agent concentration used in the injection and suggests low efficiency of the subconjunctival route to deliver hydrophilic molecules to the anterior segment of the eye. Particularly, only approximately 0.06% of the contrast agent in the injection solution was in the anterior chamber at 40 min after the injection. For transscleral delivery to the posterior segment of the eye via the subconjunctival route, no penetration of the contrast agent into the vitreous was detected *in vivo*. Instead, the majority of the hydrophilic probe was delivered from the subconjunctival depot to the surrounding tissues of the eye. A clearance pathway from the subconjunctival depot to the region near the periocular fat behind the eye was also observed for the hydrophilic probe. In the present intravitreal delivery study, different from previous observations, noticeable concentration of the contrast agent was observed in the anterior chamber when higher contrast agent concentration was used in the intravitreal injection. The contrast agent concentration in the anterior chamber was determined to be approximately 10% of that in the vitreous. This suggests that the anterior clearance route after intravitreal injection can be important for the clearance of small hydrophilic molecules. Besides the anterior route, other vitreal clearance routes were also observed: the contrast agent was found in the optic nerve, albeit at low concentration, and in the tissues surrounding the eye after intravitreal injection. These present findings provide insights into ocular pharmacokinetics of hydrophilic molecules in ocular delivery that could serve as basic knowledge to pharmaceutical scientists for the design of more effective ocular drug delivery systems. The results in the present study also demonstrate that the high contrast agent concentration approach could improve the visualization of the penetration and clearance pathways in MRI pharmacokinetic studies of ocular delivery.

Acknowledgments

This research was supported by National Institutes of Health (NIH) Grant EY 015181. The content is solely the responsibility of the authors and does not necessarily represent the official views of National Eye Institute or NIH. The authors thank He Wen for her help in the preparation of the experiments, Tamara Davis and Robin Casagrande for their assistance in MRI, and Dr. Debra Kemper, Dr. Dawn Forste, Carissa Lester, Liz Roselle, and Holly Chafin for their help in animal handling, and Dr. Eun-Kee Jeong for helpful discussion.

References

1. Li SK, Lizak MJ, Jeong EK. MRI in ocular drug delivery. NMR Biomed. 2008; 21(9):941–956. [PubMed: 18186077]
2. Kim H, Robinson MR, Lizak MJ, Tansey G, Lutz RJ, Yuan P, Wang NS, Csaky KG. Controlled drug release from an ocular implant: An evaluation using dynamic three-dimensional magnetic resonance imaging. Invest Ophthalmol Vis Sci. 2004; 45(8):2722–2731. [PubMed: 15277497]
3. Kim SH, Csaky KG, Wang NS, Lutz RJ. Drug elimination kinetics following subconjunctival injection using dynamic contrast-enhanced magnetic resonance imaging. Pharm Res. 2008; 25(3): 512–520. [PubMed: 17674155]

4. Li SK, Jeong EK, Hastings MS. Magnetic resonance imaging study of current and ion delivery into the eye during transscleral and transcorneal iontophoresis. Invest Ophthalmol Vis Sci. 2004; 45(4): 1224–1231. [PubMed: 15037591]
5. Li SK, Molokhia SA, Jeong EK. Assessment of subconjunctival delivery with model ionic permeants and magnetic resonance imaging. Pharm Res. 2004; 21(12):2175–2184. [PubMed: 15648248]
6. Molokhia SA, Jeong EK, Higuchi WI, Li SK. Examination of penetration routes and distribution of ionic permeants during and after transscleral iontophoresis with magnetic resonance imaging. Int J Pharm. 2007; 335(1–2):46–53. [PubMed: 17236728]
7. Molokhia SA, Jeong EK, Higuchi WI, Li SK. Examination of barriers and barrier alteration in transscleral iontophoresis. J Pharm Sci. 2008; 97(2):831–844. [PubMed: 17879296]
8. Molokhia SA, Jeong EK, Higuchi WI, Li SK. Transscleral iontophoretic and intravitreal delivery of a macromolecule: Study of ocular distribution *in vivo* and postmortem with MRI. Exp Eye Res. 2009; 88(3):418–425. [PubMed: 19000673]
9. Shi X, Liu X, Wu X, Lu ZR, Li SK, Jeong EK. Ocular pharmacokinetic study using T_1 mapping and Gd-chelate-labeled polymers. Pharm Res. 2011; 28(12):3180–3188. [PubMed: 21691891]
10. Jockovich ME, Murray TG, Clifford PD, Moshfeghi AA. Posterior juxtascleral injection of anecortave acetate: Magnetic resonance and echographic imaging and localization in rabbit eyes. Retina. 2007; 27(2):247–252. [PubMed: 17290209]
11. Kim H, Lizak MJ, Tansey G, Csaky KG, Robinson MR, Yuan P, Wang NS, Lutz RJ. Study of ocular transport of drugs released from an intravitreal implant using magnetic resonance imaging. Ann Biomed Eng. 2005; 33(2):150–164. [PubMed: 15771269]
12. Wood GK, Berkowitz BA, Wilson CA. Visualization of subtle contrast-related intensity changes using temporal correlation. Magn Reson Imaging. 1994; 12(7):1013–1020. [PubMed: 7997088]
13. Kalavagunta C, Metzger GJ. A field comparison of r1 and r2* relaxivities of Gd-DTPA in aqueous solution and whole blood: 3T versus 7T. Proc Int Soc Magn Reson Med. 2010; 18:4990.
14. Koenig SH, Kellar KE. Blood-pool contrast agents for MRI: A critical evaluation. Acad Radiol. 1998; 5(Suppl 1):S200–S205. [PubMed: 9561081]
15. Pintaske J, Martirosian P, Graf H, Erb G, Lodemann KP, Claussen CD, Schick F. Relaxivity of gadopentetate dimeglumine (Magnevist), gadobutrol (Gadovist), and gadobenate dimeglumine (MultiHance) in human blood plasma at 0.2, 1.5, and 3 Tesla. Invest Radiol. 2006; 41(3):213–221. [PubMed: 16481903]
16. Kadam RS, Cheruvu NP, Edelhauser HF, Kompella UB. Sclera-choroid-RPE transport of eight beta-blockers in human, bovine, porcine, rabbit, and rat models. Invest Ophthalmol Vis Sci. 2011; 52(8):5387–5399. [PubMed: 21282583]
17. Wen H, Hao J, Li SK. Influence of permeant lipophilicity on permeation across human sclera. Pharm Res. 2010; 27(11):2446–2456. [PubMed: 20734114]
18. Robinson MR, Lee SS, Kim H, Kim S, Lutz RJ, Galban C, Bungay PM, Yuan P, Wang NS, Kim J, Csaky KG. A rabbit model for assessing the ocular barriers to the transscleral delivery of triamcinolone acetonide. Exp Eye Res. 2006; 82(3):479–487. [PubMed: 16168412]
19. Lee SS, Robinson MR. Novel drug delivery systems for retinal diseases. A review. Ophthalmic Res. 2009; 41(3):124–135. [PubMed: 19321933]
20. Lee SJ, He W, Robinson SB, Robinson MR, Csaky KG, Kim H. Evaluation of clearance mechanisms with transscleral drug delivery. Invest Ophthalmol Vis Sci. 2010; 51(10):5205–5212. [PubMed: 20484583]
21. Weijtens O, van der Sluijs FA, Schoemaker RC, Lentjes EG, Cohen AF, Romijn FP, van Meurs JC. Peribulbar corticosteroid injection: Vitreal and serum concentrations after dexamethasone disodium phosphate injection. Am J Ophthalmol. 1997; 123(3):358–363. [PubMed: 9063245]
22. Bron AJ, Richards AB, Knight-Jones D, Easty DL, Ainslie D. Systemic absorption of Soframycin after subconjunctival injection. Br J Ophthalmol. 1970; 54(9):615–620. [PubMed: 5458253]
23. Lee TW, Robinson JR. Drug delivery to the posterior segment of the eye: Some insights on the penetration pathways after subconjunctival injection. J Ocul Pharmacol Ther. 2001; 17(6):565–572. [PubMed: 11777180]

24. Steel DH, Thorn J. The incidence of systemic side-effects following subconjunctival Mydricaine no. 1 injection. Eye (Lond). 1999; 13(Pt 6):720–722. [PubMed: 10707131]
25. Tsuji A, Tamai I, Sasaki K. Intraocular penetration kinetics of prednisolone after subconjunctival injection in rabbits. Ophthalmic Res. 1988; 20(1):31–43. [PubMed: 3380524]
26. Maurice D. Review: Practical issues in intravitreal drug delivery. J Ocul Pharmacol Ther. 2001; 17(4):393–401. [PubMed: 11572470]
27. Urtti A. Challenges and obstacles of ocular pharmacokinetics and drug delivery. Adv Drug Deliv Rev. 2006; 58(11):1131–1135. [PubMed: 17097758]
28. Nair G, Pardue MT, Kim M, Duong TQ. Manganese-enhanced MRI reveals multiple cellular and vascular layers in normal and degenerated retinas. J Magn Reson Imaging. 2011; 34(6):1422–1429. [PubMed: 21964629]
29. Thuen M, Olsen O, Berry M, Pedersen TB, Kristoffersen A, Haraldseth O, Sandvig A, Brekken C. Combination of Mn^{2+}-enhanced and diffusion tensor MR imaging gives complementary information about injury and regeneration in the adult rat optic nerve. J Magn Reson Imaging. 2009; 29(1):39–51. [PubMed: 19097077]
30. Watanabe T, Michaelis T, Frahm J. Mapping of retinal projections in the living rat using high-resolution 3D gradient-echo MRI with Mn^{2+}-induced contrast. Magn Reson Med. 2001; 46(3): 424–429. [PubMed: 11550231]
31. Kim SH, Galban CJ, Lutz RJ, Dedrick RL, Csaky KG, Lizak MJ, Wang NS, Tansey G, Robinson MR. Assessment of subconjunctival and intrascleral drug delivery to the posterior segment using dynamic contrast-enhanced magnetic resonance imaging. Invest Ophthalmol Vis Sci. 2007; 48(2): 808–814.10.1002/jps [PubMed: 17251481]
32. Liu X, Li SK, Jeong EK. Ocular pharmacokinetic study of a corticosteroid by 19F MR. Exp Eye Res. 2010; 91(3):347–352. [PubMed: 20537996]
33. Heinrich MC, Kuhlmann MK, Kohlbacher S, Scheer M, Grgic A, Heckmann MB, Uder M. Cytotoxicity of iodinated and gadolinium-based contrast agents in renal tubular cells at angiographic concentrations: In vitro study. Radiology. 2007; 242(2):425–434. [PubMed: 17179401]
34. Cacheris WP, Quay SC, Rocklage SM. The relationship between thermodynamics and the toxicity of gadolinium complexes. Magn Reson Imaging. 1990; 8(4):467–481. [PubMed: 2118207]
35. Ersoy H, Rybicki FJ. Biochemical safety profiles of gadolinium-based extracellular contrast agents and nephrogenic systemic fibrosis. J Magn Reson Imaging. 2007; 26(5):1190–1197. [PubMed: 17969161]
36. Tomita M, Hayashi M, Awazu S. Absorption-enhancing mechanism of EDTA, caprate, and decanoylcarnitine in Caco-2 cells. J Pharm Sci. 1996; 85(6):608–611. [PubMed: 8773957]
37. Berkowitz BA, Roberts R, Luan H, Peysakhov J, Mao X, Thomas KA. Dynamic contrast-enhanced MRI measurements of passive permeability through blood retinal barrier in diabetic rats. Invest Ophthalmol Vis Sci. 2004; 45(7):2391–2398. [PubMed: 15223822]
38. Dumas S, Jacques V, Sun WC, Troughton JS, Welch JT, Chasse JM, Schmitt-Willich H, Caravan P. High relaxivity magnetic resonance imaging contrast agents. Part 1. Impact of single donor atom substitution on relaxivity of serum albumin-bound gadolinium complexes. Invest Radiol. 2010; 45(10):600–612. [PubMed: 20808235]
39. Powell DH, Ni Dhubhghaill OM, Pubanz D, Helm L, Lebedev YS, Schlaepfer W, Merbach AE. Structural and dynamic parameters obtained from ^{17}O NMR, EPR and NMRD studies of monomeric and dimeric Gd^{3+} complexes of interest in magnetic resonance imaging: An integrated and theoretically self-consistent approach. J Am Chem Soc. 1996; 118(39):9333–9346.

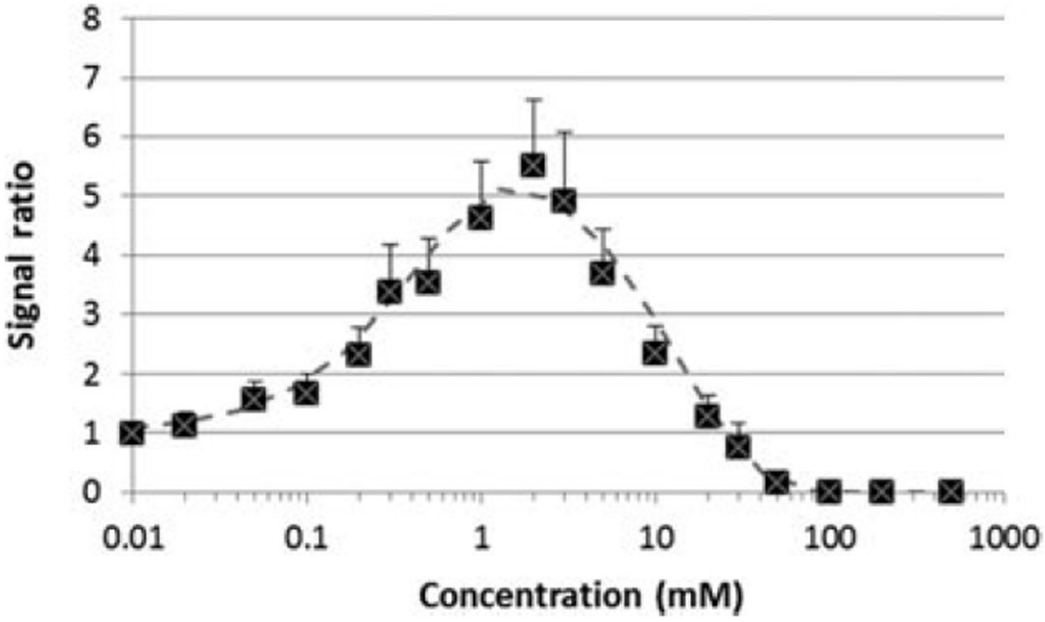

Figure 1.
Ratios of MR signals of Gd–DTPA solutions to that of saline as a function of Gd–DTPA concentration obtained with the 3-T MRI scanner. Symbols, experimental data; curve, best-fit line for the data using Eqs. 1-3.

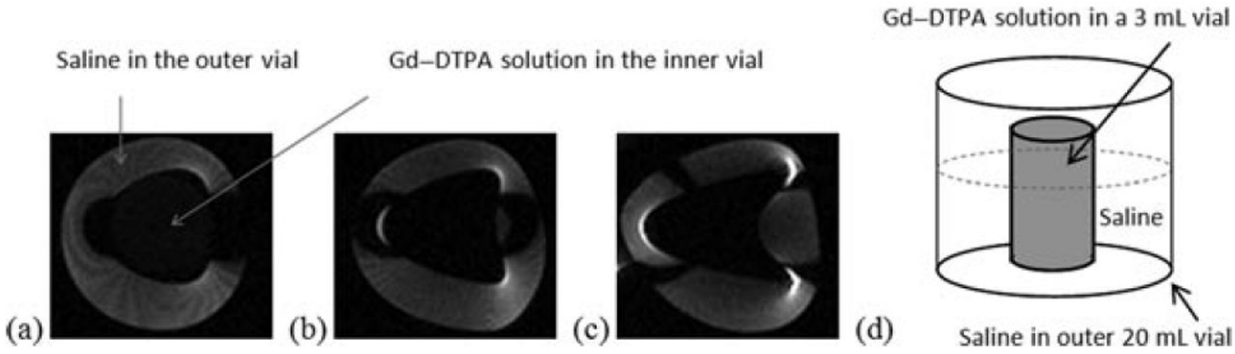

Figure 2.
Representative MR images (coronal view) of the high concentration Gd–DTPA vials in saline, illustrating the effects of magnetic susceptibility artifact at (a) 0.05 M, (b) 0.1 M, and (c) 0.2 M Gd–DTPA. (d) Diagram illustrating the vials.

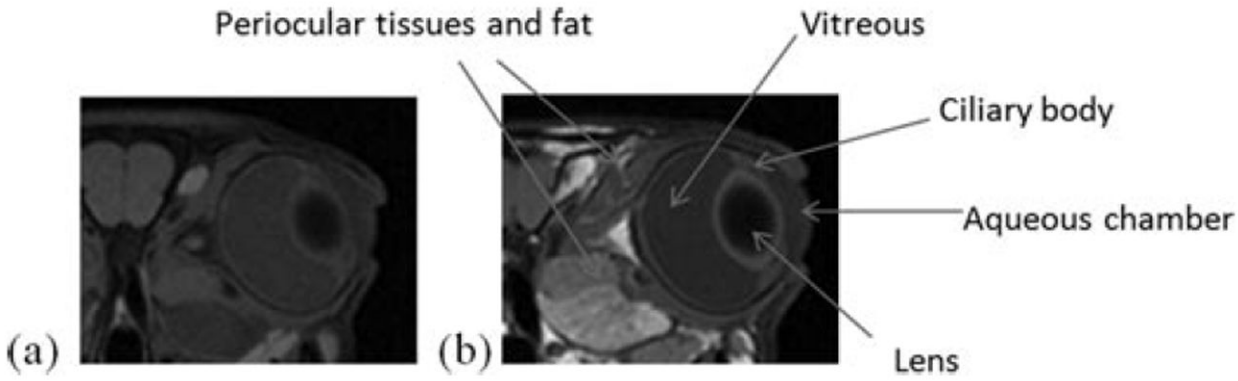

Figure 3.
MR images (axial view) of the eye before contrast agent injections (the controls) using MR sequence (a) with and (b) without fat suppression.

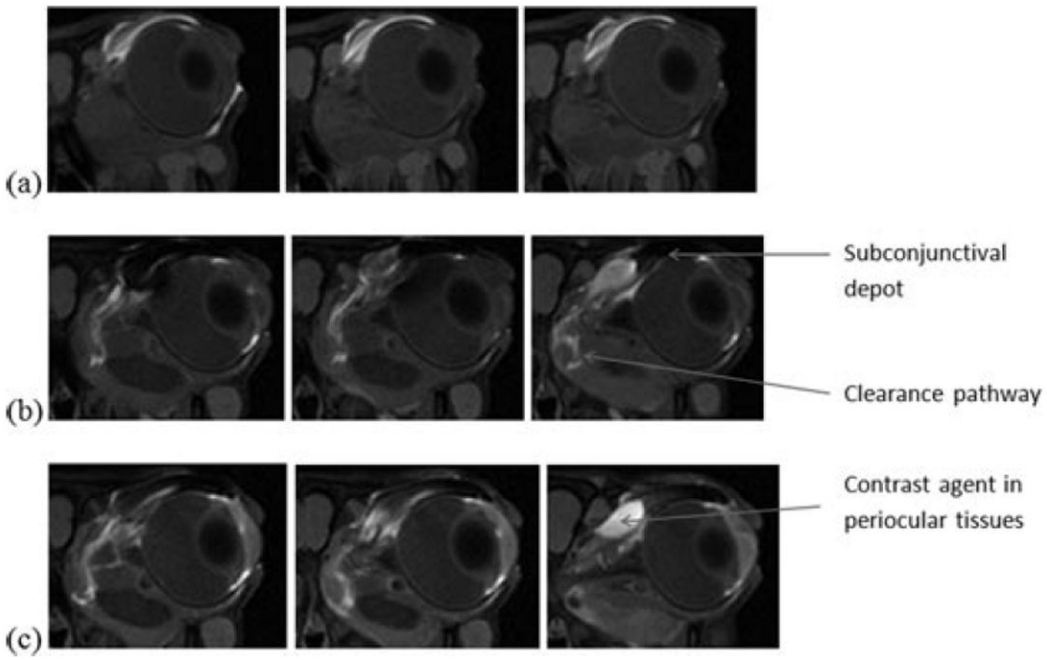

Figure 4.

Representative MR images of rabbit eyes after subconjunctival injections of Gd–DTPA at concentrations of (a) 0.05 M, and (b and c) 0.5 M *in vivo*. Images were acquired during the 16 min MR scans of (a) 27–43 min, (b) 10–26 min, and (c) 49–65 min after the injections. From left to right, axial image slices at different positions from the front to the back of the head.

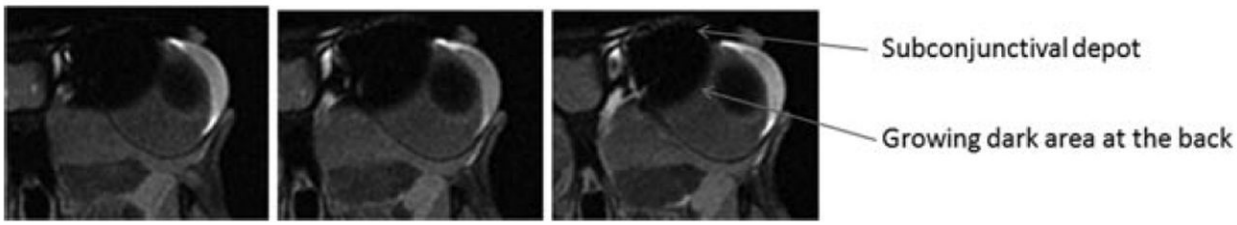

Figure 5.
Representative MR images of rabbit eyes after subconjunctival injections of Gd–DTPA at concentration of 0.5 M postmortem. Images were acquired during the 16 min MR scan of 35–51 min after the injection. From left to right, axial image slices at different positions from the front to the back of the head.

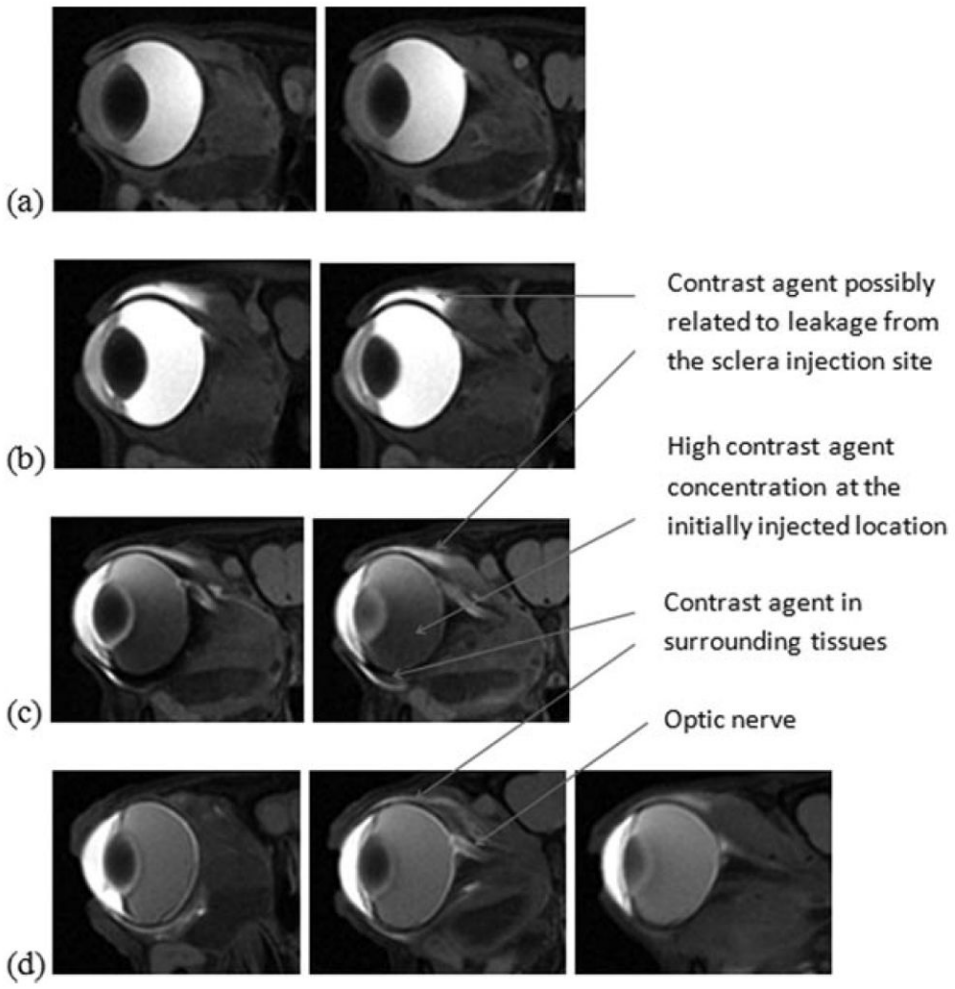

Figure 6.
Representative MR images in the intravitreal injection studies of Gd–DTPA at concentrations of (a) 0.005 M, (b) 0.05 M, and (c and d) 0.5 M *in vivo*, acquired at (a, b, and c) 4 h and (d) 12 h after the injections. From left to right, axial image slices at different positions from the front to the back of the head.